HHS Public Access

Author manuscript

Nat Chem Biol. Author manuscript; available in PMC 2013 August 01.

Published in final edited form as:

Nat Chem Biol. 2013 February ; 9(2): 97–104. doi:10.1038/nchembio.1136.

Whole-organism screening for gluconeogenesis identifies activators of fasting metabolism

Philipp Gut[1,*], **Bernat Baeza-Raja**[2], **Olov Andersson**[1,6], **Laura Hasenkamp**[1], **Joseph Hsiao**[1], **Daniel Hesselson**[1,7], **Katerina Akassoglou**[2], **Eric Verdin**[3,4], **Matthew D. Hirschey**[3,4,5], and **Didier Y.R. Stainier**[1,8,*]

[1]Department of Biochemistry and Biophysics, Programs in Developmental and Stem Cell Biology, Genetics and Human Genetics, the Diabetes Center, Institute for Regeneration Medicine and Liver Center, University of California, San Francisco, 1550 4th Street, San Francisco, CA 94158, USA

[2]The Gladstone Institute of Neurological Disease, San Francisco, CA 94158, USA

[3]The Gladstone Institute of Virology and Immunology, San Francisco, CA 94158, USA

[4]Department of Medicine, University of California, San Francisco, California 94143, USA

[5]Sarah W. Stedman Nutrition and Metabolism Center and the Departments of Medicine and Pharmacology & Cancer Biology, Duke University Medical Center, Durham, NC, 27710, USA

Abstract

Improving the control of energy homeostasis can lower cardiovascular risk in metabolically compromised individuals. To identify new regulators of whole-body energy control, we conducted a high-throughput screen in transgenic reporter zebrafish for small molecules that modulate the expression of the fasting-inducible gluconeogenic gene *pck1*. We show that this *in vivo* strategy identified several drugs that impact gluconeogenesis in humans, as well as metabolically uncharacterized compounds. Most notably, we find that the Translocator Protein (TSPO) ligands PK 11195 and Ro5-4864 are glucose lowering agents despite a strong inductive effect on *pck1* expression. We show that these drugs are activators of a fasting-like energy state, and importantly that they protect high-fat diet induced obese mice from hepatosteatosis and glucose intolerance,

[*]Corresponding authors: Philipp Gut, philipp.gut@ucsf.edu, Phone: (415) 420-1564. Didier Y.R. Stainier, didier.stainier@mpi-bn.mpg.de, Phone: 49 6032-705-1301.

[6]Current address: Department of Cell and Molecular Biology, Karolinska Institute, 17177 Stockholm, Sweden

[7]Current address: Garvan Institute of Medical Research, Diabetes and Obesity Research Program, 384 Victoria Street, Darlinghurst, NSW, 2010, Australia

[8]Current address: Department of Developmental Genetics, Max Planck Institute for Heart and Lung Research, Bad Nauheim, Germany

AUTHOR CONTRIBUTIONS

P.G. conceived the study, designed and performed experiments, analyzed data and wrote the paper. D.Y.R.S. designed experiments, analyzed data, supervised the work and wrote the paper. M.D.H. designed and performed experiments, and analyzed data. O.A., B.B.-R., D.H., L.H. and J.H. performed experiments. K.A. and E.V. contributed material and supervised the work. All authors commented on the paper.

COMPETING FINANCIAL INTERESTS

The authors declare no competing financial interest.

two pathological manifestations of metabolic dysregulation. Thus, using a whole-organism screening strategy, this study has identified new small molecule activators of fasting metabolism.

INTRODUCTION

Cardiovascular disease is the primary cause of death worldwide[1]. Metabolic disorders like obesity and type 2 diabetes, which constitute major risk factors for cardiovascular pathogenesis[2], lead to a poor control of energy homeostasis. The resulting chronic hyperlipidemia and hyperglycemia can further contribute to insulin resistance and the loss of metabolic flexibility towards changes in nutrient availability. Ultimately, aberrant lipid accumulation occurs in several organs and has deleterious consequences[3,4]. Current drug discovery strategies focus on molecules that can function on diverse pathogenic modalities of metabolic disease by shifting the impaired energy control of a metabolically ill individual towards that of a metabolically healthy person[5,6]. Despite vigorous academic and industrial efforts, discovery and development of new lead compounds for the amelioration of metabolic diseases remain ineffective. The slow progress reflects complex inter-organ feedback circuits that regulate the behavior and metabolic management of energy intake, storage and expenditure. In addition, biotransformation and xenobiotic defense of different organs influence the pharmaco-dynamics and -kinetics of chemical agents in a living organism. These complexities set high bars for extrapolating drug-target interactions *in vitro* to pharmacological actions *in vivo*, and many drugs that are identified in target-based screening approaches ultimately fail[7,8]. Taking these challenges into consideration, it becomes evident that developing rapid, cost efficient and translational small molecule discovery and metabolic profiling technologies in whole organisms is necessary to identify effective therapeutics.

Here, we report on an innovative drug discovery strategy in larval zebrafish for the identification of metabolically active drugs with potential therapeutic function. Zebrafish have proven to be a powerful model for phenotype-based small molecule screening that can be translated into mammalian pharmacology[9]. In addition, fundamental principles of energy homeostasis are evolutionary conserved in metazoans[10]. We leveraged zebrafish yolk consumption to pharmacologically profile pathways of energy control; When yolk-derived carbohydrates become depleted, zebrafish initiate a gluconeogenic program to match glucose demand for organ function and organismal survival. This gluconeogenic ‘feeding to fasting’ switch can be monitored in thousands of larvae per experimental day without additional variables, such as an external nutrient supply. At this stage, zebrafish larvae have developed functional organs, and they are still small enough to be assayed in a high-throughput 96-well plate format. Furthermore, zebrafish can be easily treated with drugs, and their transparency allows direct microscopic evaluation of organ morphology as well as general health.

Based on these characteristics, we developed and applied a drug discovery approach that rapidly interrogates small molecules on their ability to interfere with gluconeogenesis and its homeostatic control. For fast quantitative and visual monitoring of gluconeogenesis, we generated transgenic bioluminescence and fluorescence reporter zebrafish using the

cytosolic phosphoenolpyruvate-carboxykinase (*pck1*) promoter. *pck1* is a prototypical fasting responsive gene: when dietary carbohydrates are low after prolonged fasting, *pck1* is induced transcriptionally and its protein product catalyzes a regulatory step in gluconeogenesis by mediating the conversion of tricarboxylic acid (TCA) cycle-derived oxaloacetate to phosphoenolpyruvate and carbon dioxide in the liver and kidney. The resulting phosphoenolpyruvate is used as the starting substrate for gluconeogenesis. *pck1* transcription is under insulin control during feeding conditions, and under glucagon, glucocorticoids and adrenaline control during fasting conditions[11,12]. Murine *Pck1* promoter activity and mRNA abundance correlates with protein mass and enzymatic activity levels[13]. In this paper, we developed a *pck1* reporter that captures the properties of its regulatory elements, and used it in a small molecule screen. We identified several known pharmacological modulators of *pck1* expression as well as compounds not previously identified as metabolic regulators. Two of these compounds, the Transporter Protein (TSPO) ligands PK 11195 and Ro5-4864, surprisingly reduce glucose levels while increasing *pck1* expression. Importantly, we show that PK 11195 promotes health in diet-induced obese mice, validating the zebrafish data in a mammalian system and building a framework to develop a new class of drugs for metabolic diseases.

RESULTS

Monitoring gluconeogenesis in larval zebrafish

The yolk of zebrafish larvae is fully depleted between 4 and 5 dpf (Supplementary Results, Supplementary Fig. 1). In response to this ‘feeding to fasting’ transition, zebrafish larvae activate the transcription of the prototypical fasting-inducible gluconeogenic gene *pck1* (Supplementary Fig. 2a). We generated *pck1* reporter zebrafish to monitor this transcriptional activation of *pck1* as a molecular marker for the physiological switch towards fasting (Fig. 1a and Supplementary Fig. 2b). For rapid, quantitative assessment of *pck1* promoter activity, the firefly luciferase gene *Luc2* was cloned downstream of a 2.8kb *pck1* promoter fragment. In addition, a second zebrafish transgenic line was generated using a yellow fluorescent protein (Venus) in order to image the *pck1* response and liver morphology with cellular resolution. To facilitate the identification of the luciferase transgenic animals, we incorporated in the transgene a *cryaa:mcherry* cassette, which results in a constitutive red eye signal as early as 48 hours post fertilization (hpf)[14] (Supplementary Fig. 2c). As expected, we observed *pck1* promoter activity in the *Tg(pck1:Venus,cryaa:mcherry)*^{s953} [hereafter named *Tg(pck1:Venus)*] zebrafish in tissues that correspond to mammalian organs with well documented gluconeogenic activity, including the liver and pronephros (Fig. 1a, Supplementary Fig. 2d). The transgenic reporter’s spatial and temporal expression pattern was identical to that of endogenous *pck1*, as detected with antisense riboprobes (Fig. 1a and Supplementary Fig. 2a), thereby validating the use of this transgenic zebrafish reporter line to monitor endogenous gene expression.

To quantify the induction of *pck1* expression, we used the bioluminescence reporter line *Tg(pck1:Luc2,cryaa:mcherry)*^{s952} [hereafter named *Tg(pck1:Luc2)*], and detected a 36-fold incremental activation of the *pck1* promoter during the progression of yolk depletion and

transition into a caloric deficit between 3 and 7 dpf. The time course of *pck1* induction correlated with an initial increase in free glucose levels, followed by a loss of glucose, likely in response to net depletion of gluconeogenic substrates in never fed larvae (Fig. 1b). Thus, the analysis of these transgenic reporters confirms that fasting zebrafish larvae exhibit a transcriptional gluconeogenic response similar to that seen during a feeding to fasting transition in mammals[15].

Next, we designed a high-throughput platform to screen for compounds that modulate *pck1* promoter activity. Three 4 dpf *Tg(pck1:Luc2)* zebrafish larvae were distributed in each well of a 96-well plate. After 48 hours, we visually assessed larval health and morphology and then added a long half-life firefly luciferin to measure bioluminescence directly. Using this assay, we first addressed the evolutionary conservation and tested the dynamic range of *pck1* promoter activity in zebrafish treated with known pharmacological modulators of human gluconeogenesis. We tested the beta-adrenergic agonist isoprenaline, an inducer of gluconeogenesis, and the anti-diabetic drug metformin, an indirect AMP-activated protein kinase (AMPK) activator, which suppresses gluconeogenesis[16,17,18]. While metformin by itself resulted in only a mild reduction of *pck1* promoter activity, it lowered both *pck1* promoter activity and free glucose levels in isoprenaline-stimulated animals (Fig. 1c,d and Supplementary Figure 3). Thus, the gluconeogenic response to fasting in zebrafish and its pharmacological modulation with known drugs are sufficiently similar to those in mammals to support the use of this model system as a tool for metabolic drug discovery.

A whole-organism screen for modulators of gluconeogenesis

To identify new regulators of metabolic homeostasis, we performed a small molecule screen for modulators of gluconeogenesis. In total, we tested 2400 bioactive compounds for their ability to modulate *pck1* promoter activity (Fig. 2a). After a 48h incubation, we evaluated zebrafish morphology and general health to exclude toxic compounds before assaying Luciferase activity. The workflow of the primary screen is described in detail in Supplementary Figure 4. We further selected 60 compounds representing different drug classes and analyzed their effect on whole larva glucose levels. Table 1 shows a partial list of drugs that significantly affected *pck1* promoter activity as well as their effects on glucose levels. Among these drugs, we found well-characterized regulators of glucose homeostasis and cardiovascular risk in humans. For example, synthetic glucocorticoids are widely prescribed anti-inflammatory agents but are known to cause diabetes through promoting hepatic glucose production. We found several glucocorticoids that induced zebrafish *pck1* promoter activity and led to high glucose levels, compatible with activated gluconeogenesis. In addition, beta-adrenergic agonists as well as multiple psychoactive drugs with known adverse effects on metabolism increased *pck1* promoter activity and glucose levels (Fig. 2b, Table 1). The combination of high Luciferase activity and high glucose levels is suggestive of enhanced gluconeogenesis in response to these US Food and Drug Administration (FDA) approved drugs.

These initial findings of compounds that modulate gluconeogenesis similarly in humans and zebrafish prompted us to screen for small molecules not previously reported to modulate glucose production. We hypothesized that compounds that would enhance *pck1* promoter

activity while lowering whole-body glucose levels are not direct activators of gluconeogenesis, but instead trigger compensatory gluconeogenic responses to replenish depleted carbohydrates. Furthermore, small molecules that lower glucose levels while increasing *pck1* promoter activity might stimulate energy expenditure. Only 2 of 60 compounds that induced *Tg(pck1:*Luc2*)* levels also led to this unique low glucose phenotype. We found that PK 11195 (**1**), a selective TSPO ligand, reduces glucose levels while strongly enhancing *pck1* promoter activity (Fig. 2b, Table 1). This isoquinoline-carboxamide compound induces the death of cancer cells when they are cultured in nutrient free medium, but is non-toxic when they are cultured in regular medium, suggesting a metabolic regulatory role for this drug[19]. Hence, we set out to further investigate the possibility that PK 11195 is an uncharacterized chemical compound that regulates cellular metabolism *in vivo*.

TSPO ligands enhance *pck1* and lower glucose levels

The general health of zebrafish larvae was not affected by PK 11195 treatment as we observed unaltered body morphology and liver size in *Tg(pck1:Venus)* reporter zebrafish (Supplementary Figure 5). Next, we evaluated the effects of chronic PK 11195 administration during the 'yolk feeding to fasting' transition from 4 to 7dpf. As observed in the initial screen, PK 11195 treatment robustly reduced glucose levels at all time points (Fig. 3a) while *pck1* promoter activity was increased up to 6.6-fold compared to controls (Fig. 3b). This time course analysis shows that the low glucose levels detected at 6 dpf are not due to an initial glucose peak followed by a drop in glucose levels after depletion of gluconeogenic resources, suggesting a primary glucose lowering effect of PK 11195. To analyze the structural requirements of the glucose lowering and *pck1* inducing actions of PK 11195, we tested the effects of a structural derivative of PK 11195, 1-Phenylisoquinoline-3-carboxamide (**2**) (hereafter named PKD1 for PK-Derivative 1), and a structurally unrelated high-affinity TSPO ligand, the benzodiazepine derivative Ro5-4864 (**3**) (4′-Chlorodiazepam)[20] (Fig. 3c). All three compounds enhanced Luciferase activity while decreasing glucose levels in zebrafish larvae. Co-treatment with the catecholamine analogue isoprenaline led to a synergistic induction of *Tg(pck1:*Luc2*)* activity. Importantly, the increase in glucose levels induced by isoprenaline treatment was completely reversed by PK 11195, PKD1 and Ro5-4864 treatments (Fig. 3d,e), suggesting that TSPO ligands are glucose lowering agents, even in the context of a strong gluconeogenic stimulation. These data show that PK 11195, its derivative PKD1 and the structurally unrelated TSPO ligand Ro5-4864, potently reduce whole-organism glucose levels. To test for target selectivity, we treated zebrafish larvae with Clonazepam (**4**), a benzodiazepine that has been shown to bind TSPO with low affinity (K_i of 12.9μM for replacement of radiolabeled Ro5-4864 from TSPO[21,22]). Dose response curves for Ro5-4864, PK 11195 and Clonazepam are presented in Figures 3f and g and Supplementary Table 2. As expected, Clonazepam showed a strongly reduced activity on *pck1* promoter activity and glucose levels compared to Ro5-4864 and PK 11195. To further explore TSPO as the potential target of the metabolic effects of its ligands, we analyzed expression levels *of tspo/Tspo* in the livers of zebrafish larvae and adult mice using real-time qPCR. We found *tspo/Tspo* to be expressed in the liver of both species at an expression level similar to that of other genes of metabolic control like *cpt1a/Cpt1a*, *ucp2/Ucp2* and *trib3/Trib3* (Supplementary Figure 6). Thus, we hypothesize

that the reduction in glucose levels induced by TSPO ligands is the primary drug effect, and that a homeostatic fasting response to glucose depletion explains the resulting high *Tg(pck1:*Luc2*)* activity.

PK 11195 induces key regulators of fasting

To test the above stated hypothesis, and to determine whether TSPO ligands induce a fasting-like response in hepatocytes that extends beyond the induction of gluconeogenic genes, we carried out a microarray analysis on micro-dissected liver tissue of control and PK 11195 treated 6 dpf zebrafish. To assess specifically the fasting-related molecular signature in response to PK 11195 treatment, we analyzed the activation of the peroxisome proliferator-activated receptor α (Ppar-α) target genes. Ppar-α is a canonical mediator of the adaptive response to fasting in the mammalian liver[23,24]. First, based on literature as well as mouse and human databases, we defined a gene set of known Ppar-α/PPAR-α targets [hereafter referred to as the Ppar-α target set (PTS)] and identified 82 orthologues on the zebrafish microarray chip (See **Methods and** Supplementary Table 3 for further details). Plotting of the PTS compared to all probes revealed an induction of this gene cluster (Fig. 4a). We further selected a subset of 21 members of the PTS [described as the PTS enrichment set (PES)] which are highly enriched in the top ranks of all differentially expressed genes (Fig. 4b), and most of which encode key mediators of catabolic energy metabolism. To analyze whether the induction of this gene subset represents a transcriptional response to fasting comparable to a long physiological fast in mammals, we rank-sorted all 21 PES genes within the transcriptome in 24h fasted mouse livers, followed by a cumulative distribution probability calculation. This analysis revealed that 19 out of the 21 PK 11195-induced PES genes in zebrafish are also highly enriched in the top ranks of the most up-regulated genes of 24h fasted mouse livers (P-value $<10^{-10}$ by Kolmogorov-Smirnov statistic) (Fig. 4b). These PK 11195-enriched PES genes regulate biological processes fundamentally linked to energy control including cellular bioenergetics (e.g. *alas1, nr1d1, ucp2, ucp3*), glucose metabolism (e.g. *g6pca, pck1, pgm*), beta-oxidation (e.g. *acox1, cpt1a, cpt1b, fads2*), fatty acid binding (*fabp1b.1, fabp3*) or markers of fasting with broad effects on energy metabolism (*trib3, lpin1, creb3l3*).

The close similarities between the PK 11195 response in zebrafish larvae and transcriptional changes that occur in a prolonged fast in mice, prompted us to test the effects of PK 11195 treatment in mice. To this end, we first quantified the differential expression of PES genes in PK 11195 treated zebrafish larvae. Of the 21 PES genes, we selected 10 that cover different pathways of fasting metabolism and analyzed their mRNA expression levels using real-time qPCR analysis. As expected from our previous microarray analysis, all ten genes were up-regulated in zebrafish larval livers after PK 11195 treatment (Fig. 4c).

Next, we tested whether TSPO ligands were also able to induce the same transcriptional signature in adult mice. To determine the baseline transcriptional induction of the fasting-related genes, we either fed mice ad libitum or subjected them to an 8h fast. 9 out of 10 genes of the fasting gene set were robustly induced. Strikingly, when we injected fasted mice with PK 11195, we observed a strong enhancement of the transcription of all 10 fasting-signature genes compared to vehicle-injected controls. This drug-induced

enhancement of fasting gene transcription was similar, and in some cases superior, to the induction we observed in 8h fasted mice relative to fed controls. In contrast, when mice fed ad libitum were treated with PK 11195, we could only detect a weak, and non-significant, induction of four of the fasting-related genes (Fig. 4d). However, expression of the lipogenic genes *Scd1* and *Fasn* was significantly suppressed (Supplementary Figure 7), indicating that PK 11195 treatment of fed mice triggers early-onset fasting responses, including reduced lipogenesis. Altogether, these data indicate that PK 11195 treatment activates a transcriptional response in zebrafish and mouse hepatocytes that closely resembles the gene expression changes occurring during fasting.

PK 11195 improves metabolic health in obese mice

Dietary restriction, like intermittent fasting, has been shown to exert protective effects against age-related diseases, and improves several parameters of metabolic control[25]. To address the therapeutic potential of TSPO ligands as activators of a fasting-like energy state, we tested whether PK 11195 could exert beneficial effects on high-fat diet (HFD) induced obese mice. The chronically elevated nutrient excess in this model leads to ectopic lipid accumulation and insulin resistance[4]. We hypothesized that PK 11195 as an activator of the fasting state would increase the consumption of glucose and lipids, resulting in protective effects against two key pathological features of the metabolic syndrome and diabetes: hepatosteatosis and hyperglycemia. To test for possible glucose lowering effect of PK 11195 in mice, we first subjected standard-diet fed mice to a 24h fast to deplete glycogen stores, and found that a single dose of 1mg/kg bodyweight of PK 11195 was sufficient to reduce blood glucose levels, an effect that was sustained for at least four hours after the initial injection (Standard diet; n=6; control vs. 1mg/kg bw PK 11195) (Fig. 5a). Based on these findings, we chose a low dose to assess the effects of daily PK 11195 treatments (1mg/kg bw PK 11195). We administered vehicle or PK 11195 to two independent cohorts of 5 HFD fed animals each for 5 weeks starting after 4 weeks of a high-fat feeding regimen. Histological analysis of liver tissue of PK 11195 treated mice revealed a strong reduction of lipid accumulation as assessed by Oil-Red O staining for neutral lipids and fatty acid moieties (Fig. 5b). Hematoxylin-Eosin (HE) staining revealed no histopathological characteristics of toxicity, such as hepatocyte ballooning or inflammation in PK 11195 treated mice. In accordance with the reduced lipid accumulation, we observed reduced levels of Sterol regulatory-element binding 1a (Srebp-1a), a marker of hepatosteatosis, in PK 11195 treated livers compared to controls (Fig. 5c). Serum lipid (Triglycerides, Cholesterol, LDL, HDL and Free Fatty Acids) and hormone (Insulin, Leptin) levels were largely unaffected, although we could detect a reduction of free cholesterol as well as LDL cholesterol levels in PK 11195 treated animals (Supplementary Table 4). Finally, to assess the capacity to control blood glucose levels, we challenged vehicle and PK 11195 treated animals with a glucose tolerance test after four weeks of pharmacological intervention. Whereas the control group showed the expected signs of severe glucose intolerance, indicated by a slow disposal of glucose after administration, PK 11195 treated mice displayed a significantly improved glucose tolerance (Fig. 5d). To test whether PK 11195 also exerted protective effects against fatty liver associated inflammation, we measured the mRNA levels for two pro-inflammatory cytokines, TNFα and Il-6, using real-time qPCR, and detected a strong reduction of both transcripts in the livers of the PK 11195 treatment

group (Fig. 5e). During the entire treatment period, we observed no behavioral abnormalities such as changes in fighting behavior or locomotor activity. While the food intake was similar between both groups during the 4-week period on HFD, we found a mild albeit significant reduction in weight gain in the PK 11195 treated animals compared to controls (12% weight gain vs. 20% weight gain, respectively, P=0.023) (Supplementary Figure 8). These data suggest that treatment of HFD obese mice with a relatively low dose of PK 11195 protects against hepatic steatosis and glucose intolerance – two major metabolic derangements of type 2 diabetes and the metabolic syndrome.

DISCUSSION

While testing the metabolic effects of drugs in rodents is required for drug development, high-throughput drug screening in this system is not practical. Our study describes a unique technology to discover and profile regulators of whole-body energy homeostasis using a rapid *in vivo* strategy in zebrafish. We validate our model through a small molecule screen in two ways: first, the unbiased identification of FDA approved drugs with well-conserved actions on gluconeogenesis in zebrafish and humans; second, the identification and characterization of compounds with previously unknown actions on mammalian energy homeostasis. The two chemicals identified in this study, the TSPO ligands PK 11195 and Ro5-4864, enhanced *pck1* promoter activity incrementally during the 'feeding to fasting' transition and also following isoprenaline treatment. However, in contrast to glucocorticoids or catecholamines, both ligands reduced baseline as well as isoprenaline-stimulated glucose levels. Since *Pck1* is strongly induced during fasting as part of the gluconeogenic program that replenishes glucose[12], we interpret the *pck1* inductive effect as a compensatory response to low glucose levels. Indeed, we showed that PK 11195 treatment activates transcriptional changes in the livers of zebrafish and mice that extend beyond gluconeogenesis, affecting other fasting-related adaptations like lipolysis, beta-oxidation and respiratory function. These latter two processes of energy production sustain ATP generation inside the mitochondria during low-energy states[3]. In line with this concept, the known target of PK 11195 and Ro5-4864, TSPO, is an outer mitochondrial membrane protein that has been proposed to regulate mitochondrial function[26,27]; the best defined roles of TSPO include the import of cholesterol and subsequent production of steroids and neurosteroids (e.g. dehydroepiandrosterone; DHEA), heme synthesis and transport, as well as endozepine binding[28,29]. TSPO was discovered when tissues outside the central nervous system (CNS) were found to bind [^{3}H]-Diazepam. TSPO was determined to be responsible for this binding, and therefore named peripheral benzodiazepine receptor (PBR)[30]. Ro5-4864 and PK 11195 were developed as selective and high-affinity ligands for TSPO (K_D < 10nM on rat kidney mitochondria for both ligands[21]), to try and dissect the pharmacological effects of Diazepam on the central benzodiazepine receptor ($GABA_A$) versus the peripheral benzodiazepine receptor (TSPO). Our identification of TSPO ligands as potent inducers of a fasting-like energy state opens the possibility to exploit the selectivity of these drugs to decipher their pharmacological effects on TSPO and analyze TSPO's relationship to mitochondrial biology and metabolic homeostasis. This perspective is of important clinical interest because targeting mitochondrial metabolism to improve energy homeostasis is a promising strategy to develop new anti-diabetic or anti-obesity drugs[6]. Our data show that chronic treatment of

obese mice with PK 11195 reduced markers of hepatosteatosis and significantly improved glucose tolerance. This initial characterization in a pre-diabetic disease model suggests that the TSPO ligands PK 11195 and Ro5-4864 constitute previously unappreciated chemical structures that promote metabolic health through modulation of mitochondrial function. Conclusive evidence for TSPO as the target through which these ligands modulate energy homeostasis as well as the underlying mechanisms are important avenues for future studies.

During this study, we focused our analysis on PK 11195 and Ro5-4864 to show that our approach can identify activators of a metabolic fasting response. Although the specific combination of high *pck1* expression and low glucose levels was rare among the compounds we tested, a larger profiling effort is likely to identify many more drugs with fasting-enhancing effects that act on different biological pathways. In addition to this strategy, future pharmacological profiling could also be devised to identify drugs that selectively reduce *pck1* promoter activity as well as glucose levels, indicative of decreased gluconeogenesis. Relatively few compounds tested in our primary screen reduced *pck1* promoter activity, and the suppression was modest compared to the inductive effects of several *pck1* promoter-activating drugs. This result might be due to the fact that the *pck1* expression levels are at a low baseline during larval development and that a stronger reduction is incompatible with zebrafish health. We also found that metformin, a potent suppressor of gluconeogenesis, only reduces glucose levels and *pck1* promoter activity when given in conjunction with catecholamine-induced stimulation; when given alone, it lacked a substantial effect. Hence, one approach to increase the dynamic range of the screen as well as the likelihood of identifying negative regulators of gluconeogenesis may be to screen in a sensitized background; for example, catecholamine-stimulation, a condition that simulates insulin resistance, or insulin-deficient zebrafish are attractive possibilities. In conclusion, our study provides a unique model to examine various aspects of metabolic control in a screening-accessible whole-animal vertebrate organism. This technology shows promise to bridge the gap between fast-paced high-throughput *in vitro* discovery of new drugs for metabolic diseases and the slow-paced functional *in vivo* validation in mammals.

ONLINE METHODS

Materials

Chemicals for small molecule screening were purchased as collections from Sigma and Tocris, and repurchased for validation experiments from Sigma or Tocris. 1-Phenylisoquinoline-3-carboxamide (PKD1) was purchased from Biogeneorganics (>98% purity). Ro5-4864 and Clonazepam were purchased from Sigma (>98% purity). PK 11195 was purchased from Sigma and Tocris (>98% purity). The Sigma Lopac^{1280} small molecule library contains 1,280, and the TocrisMini library 1,120 bioactive small molecules representing FDA approved drugs, bioactive research tool chemicals and natural compounds. A summary of the small molecule screening data can be found in Supplementary Table 1.

Animals and generation of transgenic zebrafish

Adult zebrafish AB or TL strains were raised at 28°C under standard laboratory conditions. Larvae were kept in 12h light cycles until treatment. Transgenic zebrafish were generated using I-SCEI meganuclease mediated transgenic insertion into one-cell stage embryos as previously described[45]. For efficient selection of carriers in absence of a signal [in *Tg(pck1:Luc2,cryaa:mCherry)* ^{s952} and before 4.5 dpf in *Tg(pck1:Venus,cryaa:mCherry)* ^{s953} reporter zebrafish] an eyemarker cassette, *cryaa:mcherry*, was cloned in reverse direction downstream of the 2.8kb *pck1* promoter fragment. The *Tg(pck1:Luc2)* reporter was used for quantification of *pck1* promoter activity and the *Tg(pck1:Venus)* reporter for visualization. One founder for each transgenic line *[Tg(pck1:Luc2,cryaa:mCherry)* ^{s952} *and Tg(pck1:Venus,cryaa:mCherry)*^{s953}] was selected and subsequent generations were propagated and expanded.

For mouse studies, ten-week old C57BL/6 male mice (The Jackson Labs) were kept with five animals per cage and were fed a high-fat diet (60% calories derived from fat, Research Diets) until 14 weeks of age. From 14 to 19 weeks, vehicle or 1 mg/kg bodyweight PK 11195 (in Saline/1% DMSO) was injected subcutaneously once per day for 5 days. Body weight and food intake were measured twice weekly. Analysis was performed on two independent cohorts of 5 controls and 5 PK 11195 treated mice each with similar results. Husbandry and experimental protocols for zebrafish and mouse studies were approved by IACUC.

In vivo luciferase reporter assay and small molecule screening

The *Tg(pck1:Luc2,cryaa:mCherry)* ^{s952} zebrafish TL line was in-crossed, raised and selected for homozygous transgenic carriers which were then outcrossed to AB wildtype zebrafish to collect large numbers of heterozygous transgenic animals for experiments. 4 dpf healthy larvae were selected and washed with 10mM HEPES buffered E3 medium before distributing three embryos in 200µl in clear bottom opaque 96-well plates. Drugs were added from a 1mM stock solution in DMSO to derive 10µM drug concentrations in 1% DMSO unless otherwise stated. After 48h of treatment the individual wells were visually screened for morphological characteristics and evidence of toxicity was noted. The clear plate bottoms were sealed with microseal films (Biorad) to allow full bioluminescence capture. To circumvent the need for manual homogenization, 100µL E3 medium was removed and 50µl steady-glo (Promega) added to the wells to disintegrate the larvae during a 1h incubation period and to generate a stable bioluminescence signal until reading. For the small molecule screen three 3 dpf larvae were tested in duplicates for every compound. Differential modulation of *pck1* promoter activity was determined by normalization to the median of the entire plate excluding the 10 most up- and down-regulated values and subsequently $\log_2$ transformed. An average of 1-fold up- or down-regulated was assigned as hit compound threshold, filtered for interest/redundancy and further tested in validation experiments and glucose level measurements.

Metabolite and Hormone Measurements

Glucose measurements were performed on 5 times 10 zebrafish larvae per condition using a fluorescence-based enzymatic detection kit (Biovision Inc.) as previously described[46]. In

brief, five replicate pools of 10 larvae were distributed in 12-well plates and incubated with vehicle or 10μM drug in 0.1% DMSO unless otherwise stated. After 48h, the larvae were collected in 2 ml microcentrifuge tubes, the water was removed and the sample was frozen on dry ice and stored at −80°C until further analysis. After thawing, 200μl PBS was added and the larvae were homogenized using a hand-held mechanical homogenizer. 15μl of each sample were used for the glucose determination fluorescence reaction and 20μl were assigned for a Luciferase assay using a standard bioluminescence plate reader with an injection device (Veritas, Promega). For mouse experiments, drug or vehicle control was injected either into the intraperitoneal cavity for acute experiments or subcutaneously for chronic experiments. Blood was collected from the tail vain, and glucose levels were determined using a hand-held glucometer (Freestyle Lite, Abbott Diabetes Care). Glucose tolerance tests in HFD mice were performed at 4 weeks after initiation of the treatment with intraperitoneal glucose injection at 2pm. Prior to the glucose challenge, mice were fasted for 6 hours from 8am to 2pm, and received injections of vehicle or PK 11195 at 8am and 1pm. PK 11195 was prepared for injection from a 50mM stock solution that was diluted in Normal Saline to generate a 2mg/kg bodyweight final concentration containing 2.04% DMSO.

Serum lipids and hormone measurements were performed at the National Mouse Metabolic Phenotyping Centers (MMPC) at Vanderbilt University. In brief, total plasma cholesterol and triglyceride were measured by standard enzymatic assays. HDL cholesterol was measured with enzymatic method after precipitation of VLDL and LDL using dextran sulfate and Mg++. Using these data LDL cholesterol was calculated using the Friedewald equation. Free fatty acids (FFA) were extracted from plasma using heptane/isopropanol. The heptane layer containing FFA was removed, plated on silica gel plates and developed in petroleum ether, ethyl ether, and acetic acid. The FFA band was scraped from the plate and FFAs were eluted with heptane/isopropanol. The solvent was removed, and the FFAs were methylated. Methylated fatty acids were then analyzed by gas chromatography. Hormone measurements were performed as double antibody/Polyethylene glycol (PEG) Radioimmunoassay following the manufacturer's protocol.

Microarray and Real Time qPCR analysis

Liver tissue was microdissected from 6 dpf *Tg(fabp10a:GFP)*^{as3} larvae[47]. RNA was extracted using a kit for small sample size RNA isolation (RNAqueos kit, Ambion). The microarray analyses were performed in duplicates from two independent experiments with approximately 20 livers (treated with 0.1% DMSO or 10μM PK 11195). RNA was processed, labeled, hybridized and scanned at Mogene, LC according to standard protocols using an Agilent chip (Agilent). Fold change analysis was calculated using the Agilent Feature Extraction followed by GeneSpring 11.5 normalization across arrays using GeneSpring default values: Percentile Shift-75%, followed by baseline transformation to median of all samples. Log_2 transformed values are represented as MA-Plot of the intensity ratio ($M = \log_2 R - \log_2 G$) compared to the average intensity [$A = 1/2 \times (\log_2 R + \log_2 G)$] in all liver genes (R=PK 11195 group; G=vehicle group). For the comparison of transcriptional changes related to fasting from the microarray data, we generated a list of known mammalian Ppar-α/PPAR-α targets (PTS) from the literature and databases[23,48,49]. We

found 82 orthologues to be present on the zebrafish affymetrix chip and used these genes for the comparison (the full list of the PTS genes can be found in Supplementary Table 3). We defined a 21 gene subset of the PTS gene cluster as the Ppar-α Enrichment set (PES) according to the following criteria: (1) average $\log_2$ intensity above the median of all genes and (2) differential expression in the 90th percentile. We used the Kolmogorov–Smirnov statistic to calculate the significance of the cumulative distribution probability of the PES gene cluster in the top ranks of the rank-sorted transcriptome of mouse livers subjected to a 24h fast.

For mouse microarrays, livers were dissected from fed and 24h fasted wildtype mice (3 months old, standard diet, n=3/condition). Microarray preparation for Affymetrix Mouse Gene 1.0 ST arrays and subsequent data normalization, statistics and analysis were performed as previously described[50]. Labeled cDNA samples were hybridized to Affymetrix Mouse Gene 1.0 ST arrays.

RNA for real time qPCR experiments in zebrafish was obtained from approximately 20 microdissected livers as described above for the microarray analysis. cDNA for qPCR experiments was generated using standard cDNA synthesis kits according to the manufacturer's instructions (Thermo Fisher) and relative expression levels were determined by SYBR green rt-qPCR (Maxima SYBR Green, Thermo Fisher; Eco Real Time PCR, Illumina). For the real-time qPCR analyses in mice, 11–12 week male C57BL/6 were either fed ad libitum or fasted for 8h from 8am to 4pm before collection of liver tissue. To compare mRNA expression levels in control and drug treated animals, mice were injected with vehicle or 5mg/kg bw PK 11195 at 8am and 2pm (and fasted for 8h or fed ad libitum as described above). Relative mRNA abundance for the mouse samples was normalized to *Cyclophilin B* as an internal standard. Zebrafish and mouse primer pairs are listed in Supplementary Table 5.

Imaging and Histology

Brightfield and fluorescence images of zebrafish were acquired using a wide-field Zeiss Z.1. inverted microscope. For comparison of fluorescence activity, the exposure time was kept constant between groups, and contrast or brightness values were not modulated during subsequent image processing. Heat colors and color keys were generated using FIJI (Image J). High-resolution imaging of *Tg(pck1:*Venus) reporter expression in the liver and pronephros was done using laser confocal imaging with a Zeiss LSM5 Pascal confocal microscope. Whole-mount in situ hybridization was performed as previously described using *pck1* anti-sense RNA probes[51]. For mouse histology studies, liver tissue was dissected and drop-fixed in fresh 4% paraformaldehyde overnight. The following day, tissues were kept in 70% EtOH for Hematoxylin-Eosin (HE) stainings or cryoprotected using a standard sucrose gradient. After cryoprotection, tissues were placed in OCT (Tissue Tek) and stored at −80°C. ORO staining was performed on 8μm cryosections from 3 different levels of the liver of each mouse (n=5/condition) and counterstained with Mayer's hematoxylin using standard protocols.

Western blotting and antibodies

Tissues were resuspended with 50 mM Tris HCl pH 7.5, 150 mM NaCl, 5 mM EDTA, 5 mM EGTA, 20 mM NaF, and 1% NP-40 and homogenized with a Tissue homogenizer (Tissue Tearor™, Biospec Products, Inc). Lysates were centrifuged at 4°C at 16000g for 15 min and supernatants were kept. Lysates (50–100 μg) were resolved by SDS-polyacrylamide gel electrophoresis (PAGE), transferred onto a polyvinylidene difluoride (PVDF) membrane (Millipore) and incubated with the following primary antibodies: Rabbit anti-SREBP1, 1:1000 (Santa Cruz Biotechnology) and mouse anti-tubulin, 1:5000 (Sigma). Rabbit immunoglobulin G-specific horseradish peroxidase antibody or mouse immunoglobulin G-specific horseradish peroxidase (Jackson) was used for detection. Quantification was performed using FIJI (Image J). A representative western blot from three independent experiments is shown.

Statistics

Results are presented as mean values ± s.e.m.. P-values < 0.05 were considered as statistically significant. For statistical analysis, a two-tailed student's t-test was applied to test rejection of the null hypothesis. Kolmogorov-Smirnov statistic was performed using R (R statistical computing version 2.13.1).

Supplementary Material

Refer to Web version on PubMed Central for supplementary material.

Acknowledgments

The authors thank Amnon Schlegel, Oliver Stone and Kaveh Ashrafi for critical reading of the manuscript, the members of the Stainier lab for technical advice throughout the project, and Ana Ayala, Milagritos Alva, Pilar Lopez Pazmino and Mark Sklar for zebrafish care. We are grateful to Caroline Miller from the Gladstone Histology Core for histological processing of mouse livers. We also thank Randy Peterson for sharing knowledge on *in vivo* bioluminescence measurements in zebrafish. This study was supported in part by a postdoctoral fellowship DFG GU 1082/101 from the German Research Foundation to P.G., grant DK59637 to the MMPC lipidlab, Pilot/Feasibility Grants from the University of California San Francisco Liver Center (P30 DK026743), Diabetes and Endocrinology Center (P30 DK063720), and National Institute of Health (NIH) Grant NS051470 to K.A., funds from the Gladstone Institutes and the Glenn Foundation for Medical Research to E.V., the American Heart Association grant 12SDG8840004 to M.D.H, NIH grant RO1 DK60322, a pilot and feasibility award from the UCSF diabetes center funded by NIH U01 DK089541, and the Packard Foundation to D.Y.R.S..

References

1. WHO Cardiovascular Disease (CVD). 2008.
2. Haslam DW, James WPT. Obesity. Lancet. 2005; 366:1197–1209. [PubMed: 16198769]
3. Muoio DM, Newgard CB. Mechanisms of disease: molecular and metabolic mechanisms of insulin resistance and beta-cell failure in type 2 diabetes. Nat Rev Mol Cell Biol. 2008; 9:193–205. [PubMed: 18200017]
4. Taubes G. Insulin resistance. Prosperity's plague. Science. 2009; 325:256–260. [PubMed: 19608888]
5. Baur JA, et al. Resveratrol improves health and survival of mice on a high-calorie diet. Nature. 2006; 444:337–342. [PubMed: 17086191]
6. Tseng YH, Cypess AM, Kahn CR. Cellular bioenergetics as a target for obesity therapy. Nat Rev Drug Discov. 2010; 9:465–482. [PubMed: 20514071]

7. Silber MB. Driving drug discovery: the fundamental role of academic labs. Sci Transl Med. 2010; 2:30cm16.
8. Swinney DC, Anthony J. How were new medicines discovered? Nat Rev Drug Discov. 2011; 10:507–519. [PubMed: 21701501]
9. Zon LI, Peterson RT. In vivo drug discovery in the zebrafish. Nat Rev Drug Discov. 2005; 4:35–44. [PubMed: 15688071]
10. Schlegel A, Stainier DYR. Lessons from 'lower' organisms: what worms, flies, and zebrafish can teach us about human energy metabolism. PLoS Genet. 2007; 3:e199. [PubMed: 18081423]
11. Yang J, Reshef L, Cassuto H, Aleman G, Hanson RW. Aspects of the control of phosphoenolpyruvate carboxykinase gene transcription. J Biol Chem. 2009; 284:27031–27035. [PubMed: 19636079]
12. Lin HV, Accili D. Hormonal regulation of hepatic glucose production in health and disease. Cell Metab. 2011; 14:9–19. [PubMed: 21723500]
13. Burgess SC, et al. Cytosolic phosphoenolpyruvate carboxykinase does not solely control the rate of hepatic gluconeogenesis in the intact mouse liver. Cell Metab. 2007; 5:313–320. [PubMed: 17403375]
14. Kurita R, et al. Suppression of lens growth by alphaA-crystallin promoter-driven expression of diphtheria toxin results in disruption of retinal cell organization in zebrafish. Dev Biol. 2003; 255:113–127. [PubMed: 12618137]
15. Liu Y, et al. A fasting inducible switch modulates gluconeogenesis via activator/coactivator exchange. Nature. 2008; 456:269–273. [PubMed: 18849969]
16. Eisenstein AB. Current concepts of gluconeogenesis. Am J Clin Nutr. 1967; 20:282–289. [PubMed: 5335797]
17. Croniger CM, et al. Mice with a deletion in the gene for CCAAT/enhancer-binding protein beta have an attenuated response to cAMP and impaired carbohydrate metabolism. J Biol Chem. 2001; 276:629–638. [PubMed: 11024029]
18. Foretz M, et al. Metformin inhibits hepatic gluconeogenesis in mice independently of the LKB1/AMPK pathway via a decrease in hepatic energy state. J Clin Invest. 2010; 120:2355–2369. [PubMed: 20577053]
19. Gonzalez-Polo RA, et al. PK11195 potently sensitizes to apoptosis induction independently from the peripheral benzodiazepin receptor. Oncogene. 2005; 24:7503–7513. [PubMed: 16091749]
20. Rupprecht R, et al. Translocator protein (18 kDa) (TSPO) as a therapeutic target for neurological and psychiatric disorders. Nat Rev Drug Discov. 2010; 9:971–988. [PubMed: 21119734]
21. Hirsch JD, Beyer CF, Malkowitz L, Loullis CC, Blume AJ. Characterization of ligand binding to mitochondrial benzodiazepine receptors. Mol Pharmacol. 1989; 35:164–172. [PubMed: 2536464]
22. Marangos PJ, Patel J, Boulenger JP, Clark-Rosenberg R. Characterization of peripheral-type benzodiazepine binding sites in brain using [3H]Ro 5-4864. Mol Pharmacol. 1982; 22:26–32. [PubMed: 6289073]
23. Rakhshandehroo M, Hooiveld G, Müller M, Kersten S. Comparative analysis of gene regulation by the transcription factor PPARalpha between mouse and human. PLoS ONE. 2009; 4:e6796. [PubMed: 19710929]
24. Kersten S, et al. Peroxisome proliferator-activated receptor alpha mediates the adaptive response to fasting. J Clin Invest. 1999; 103:1489–1498. [PubMed: 10359558]
25. Anson RM, et al. Intermittent fasting dissociates beneficial effects of dietary restriction on glucose metabolism and neuronal resistance to injury from calorie intake. Proc Natl Acad Sci USA. 2003; 100:6216–6220. [PubMed: 12724520]
26. Rupprecht R, et al. Translocator protein (18 kD) as target for anxiolytics without benzodiazepine-like side effects. Science. 2009; 325:490–493. [PubMed: 19541954]
27. Fulda S, Galluzzi L, Kroemer G. Targeting mitochondria for cancer therapy. Nat Rev Drug Discov. 2010; 9:447–464. [PubMed: 20467424]
28. Verma A, Nye JS, Snyder SH. Porphyrins are endogenous ligands for the mitochondrial (peripheral-type) benzodiazepine receptor. Proc Natl Acad Sci USA. 1987; 84:2256–2260. [PubMed: 3031675]

29. Papadopoulos V, et al. Translocator protein (18kDa): new nomenclature for the peripheral-type benzodiazepine receptor based on its structure and molecular function. Trends Pharmacol Sci. 2006; 27:402–409. [PubMed: 16822554]
30. Braestrup C, Squires RF. Specific benzodiazepine receptors in rat brain characterized by high-affinity (3H)diazepam binding. Proc Natl Acad Sci USA. 1977; 74:3805–3809. [PubMed: 20632]
31. Song Y, et al. CRTC3 links catecholamine signalling to energy balance. Nature. 2010; 468:933–939. [PubMed: 21164481]
32. Barth E, et al. Glucose metabolism and catecholamines. Crit Care Med. 2007; 35:S508–18. [PubMed: 17713401]
33. Guhan AR, et al. Systemic effects of formoterol and salmeterol: a dose-response comparison in healthy subjects. Thorax. 2000; 55:650–656. [PubMed: 10899240]
34. Patel R, et al. LXRβ is required for glucocorticoid-induced hyperglycemia and hepatosteatosis in mice. J Clin Invest. 2011; 121:431–441. [PubMed: 21123945]
35. Vegiopoulos A, Herzig S. Glucocorticoids, metabolism and metabolic diseases. Mol Cell Endocrinol. 2007; 275:43–61. [PubMed: 17624658]
36. Tulipano G, et al. Clozapine-induced alteration of glucose homeostasis in the rat: the contribution of hypothalamic-pituitary-adrenal axis activation. Neuroendocrinology. 2007; 85:61–70. [PubMed: 17374945]
37. Smith GC, Chaussade C, Vickers M, Jensen J, Shepherd PR. Atypical antipsychotic drugs induce derangements in glucose homeostasis by acutely increasing glucagon secretion and hepatic glucose output in the rat. Diabetologia. 2008; 51:2309–2317. [PubMed: 18843478]
38. Newcomer JW. Second-generation (atypical) antipsychotics and metabolic effects: a comprehensive literature review. CNS Drugs. 2005; 19 (Suppl 1):1–93. [PubMed: 15998156]
39. Joost HG, Poser W, Panten U. Inhibition of insulin release from the rat pancreas by cyproheptadine and tricyclic antidepressants. Naunyn Schmiedebergs Arch Pharmacol. 1974; 285:99–102. [PubMed: 4280021]
40. Gupta B, Shakarwal MK, Kumar A, Jaju BP. Modulation of glucose homeostasis by doxepin. Methods Find Exp Clin Pharmacol. 1992; 14:61–71. [PubMed: 1619970]
41. Pan A, et al. Use of antidepressant medication and risk of type 2 diabetes: results from three cohorts of US adults. Diabetologia. 2012; 55:63–72. [PubMed: 21811871]
42. Srinivasan S, et al. Serotonin regulates C. elegans fat and feeding through independent molecular mechanisms. Cell Metab. 2008; 7:533–544. [PubMed: 18522834]
43. Ye Z, et al. Metabolic effects of fluoxetine in adults with type 2 diabetes mellitus: a meta-analysis of randomized placebo-controlled trials. PLoS ONE. 2011; 6:e21551. [PubMed: 21829436]
44. Andersohn F, Schade R, Suissa S, Garbe E. Long-term use of antidepressants for depressive disorders and the risk of diabetes mellitus. Am J Psychiatry. 2009; 166:591–598. [PubMed: 19339356]
45. Thermes V, et al. I-SceI meganuclease mediates highly efficient transgenesis in fish. Mech Dev. 2002; 118:91–98. [PubMed: 12351173]
46. Jurczyk A, et al. Dynamic glucoregulation and mammalian-like responses to metabolic and developmental disruption in zebrafish. Gen Comp Endocrinol. 2011; 170:334–345. [PubMed: 20965191]
47. Her GM, Yeh YH, Wu JL. 435-bp liver regulatory sequence in the liver fatty acid binding protein (L-FABP) gene is sufficient to modulate liver regional expression in transgenic zebrafish. Dev Dyn. 2003; 227:347–356. [PubMed: 12815620]
48. Kanehisa M, Goto S. KEGG: kyoto encyclopedia of genes and genomes. Nucleic Acids Res. 2000; 28:27–30. [PubMed: 10592173]
49. Finck BN, et al. Lipin 1 is an inducible amplifier of the hepatic PGC-1alpha/PPARalpha regulatory pathway. Cell Metab. 2006; 4:199–210. [PubMed: 16950137]
50. Hirschey MD, et al. SIRT3 Deficiency and Mitochondrial Protein Hyperacetylation Accelerate the Development of the Metabolic Syndrome. Mol Cell. 2011; 44:177–190. [PubMed: 21856199]
51. Thisse C, Thisse B. High-resolution in situ hybridization to whole-mount zebrafish embryos. Nat Protoc. 2008; 3:59–69. [PubMed: 18193022]

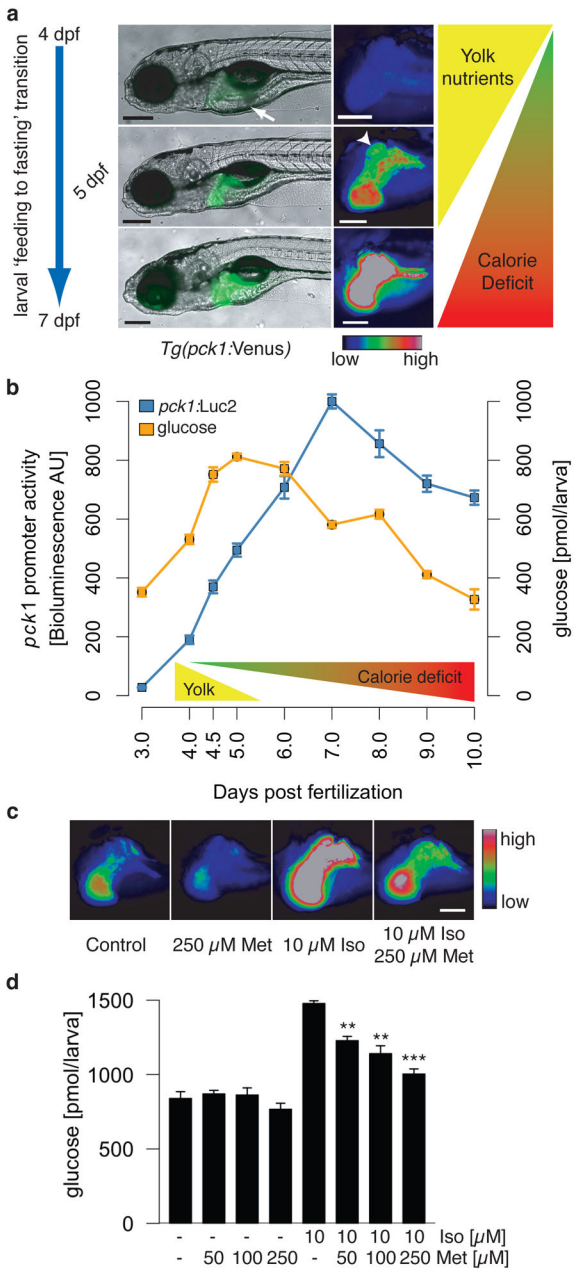

Figure 1. Rapid pharmacological profiling of gluconeogenesis

(**a**) the *pck1* promoter is activated during the larval 'feeding to fasting' transition. The arrow points to the remaining yolk at 4 dpf, which is consumed by 5 dpf. The arrowhead points to *Tg(pck1:*Venus*)* expression in the pronephros. Exposure levels during image capturing were kept constant. Black scale bars, 200μm; white scale bars, 40μM. (**b**) Time course showing glucose levels and *pck1* promoter dynamics from 3 to 10 dpf in never fed larvae. *pck1* promoter activation starts after 3 dpf and is incremental until 7 dpf. Glucose levels reach a plateau between 4.5 and 6 dpf, before the calorie deficit leads to a net depletion. (**c**) Visualization of *pck1* promoter dynamics in the liver using *Tg(pck1:Venus)* reporter zebrafish. Zebrafish larvae were treated with isoprenaline (Iso) and metformin (Met) from 4

to 6 dpf. (**d**) Glucose levels after treatment with isoprenaline and metformin (n=5×10 zebrafish/condition). **P < 0.01; ***P < 0.001; two-tailed t-test. Data are represented as mean values ± s.e.m..

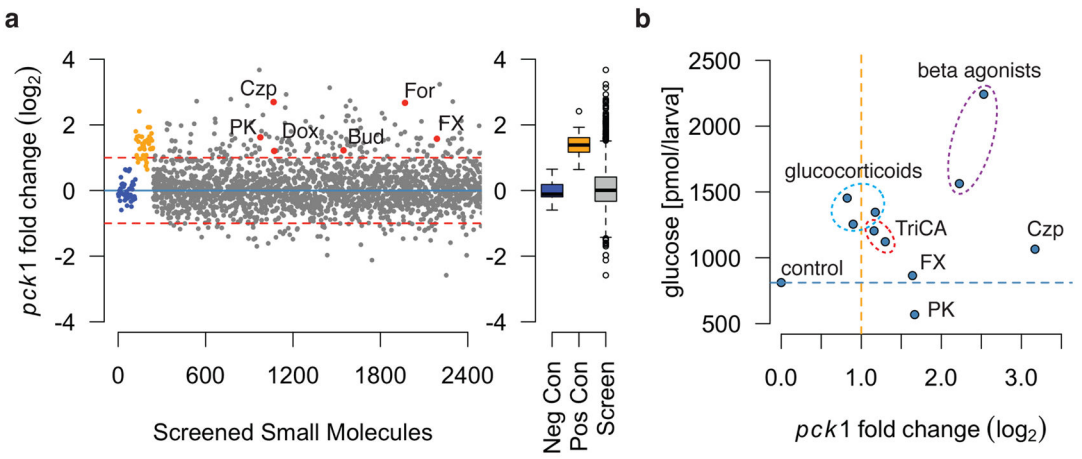

Figure 2. A small molecule screen identifies functionally conserved as well as unknown modulators of gluconeogenesis

(**a**) Differential *pck1* promoter activation by small molecules tested during the primary screen. 2400 compounds from two bioactive small molecule libraries were screened in duplicates. Neg Con = Negative Control, 1% DMSO; Pos Con = Positive Control, 10μM isoprenaline; Bud = Budenoside; Czp = Clozapine; Dox = Doxepin; For = Formoterol; FX = Fluoxetine; PK = PK 11195. (**b**) The scatterplot shows representative hit compounds found in the primary screen. FDA approved drugs that are known to influence glucose homeostasis in humans including glucocorticoids, beta-adrenergic agonists, tricyclic antidepressants (TriCA) and Czp activate *Tg(pck1:Luc2)* and increase glucose levels. Glucose concentrations are unaffected by FX and decrease after PK treatment despite high *Tg(pck1:*Luc2*)* activity suggesting compensatory gluconeogenesis (10μM from 3 to 5 dpf, P-values see Table 1). Blue dashed line indicates glucose levels of control animals. Orange dashed line indicates 1-fold $\log_2$ change of *pck1* promoter activity.

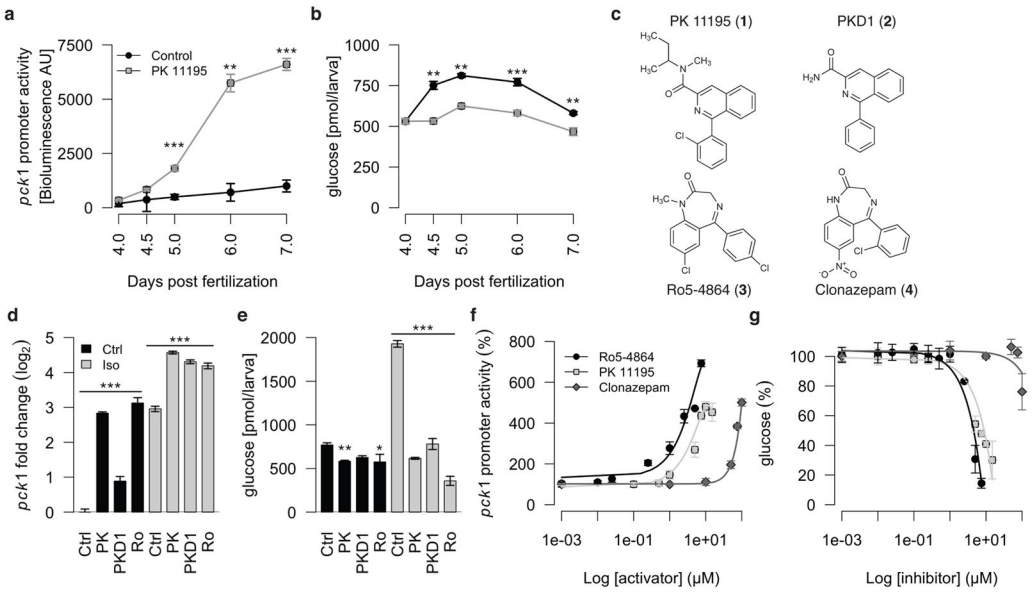

Figure 3. TSPO ligands enhance a gluconeogenic fasting response

(**a,b**) Time course analyses of *pck1* promoter activity (**a**) and glucose levels (**b**) during the 'feeding to fasting' transition in control vs. PK 11195 treated zebrafish. Glucose levels are reduced at all time points despite incrementally increasing *Tg(pck1:*Luc2*)* activity (control vs. 10μM PK 11195, 0.1% DMSO, n=5×10 larvae per condition and time point). (**c**) Structure of the TSPO ligands PK 11195, PKD1, Ro5-4864 and the benzodiazepine Clonazepam. (**d**) PK 11195, PKD1 and Ro5-4864 enhance *pck1* promoter activity and act synergistically during co-treatment with isoprenaline. (**e**) In contrast, baseline and isoprenaline stimulated glucose levels are reduced by TSPO ligand treatment [10μM isoprenaline (Iso), 10μM PK 11195 (PK), 10μM PKD1, 5μM Ro5-4864 (Ro), 0.1% DMSO; 4 to 6 dpf; n=5×10 larvae/condition]. **(f,g)** Dose-response curves of Ro5-4864, PK 11195 and Clonazepam effect on *pck1* promoter activity **(f)** and glucose levels **(g)** (stimulation with 10μM isoprenaline; 4 to 6 dpf; n = 4 × 10/condition and dilution). *P < 0.05; **P < 0.01; ***P < 0.001; two-tailed t-test. Data are represented as mean values ± s.e.m..

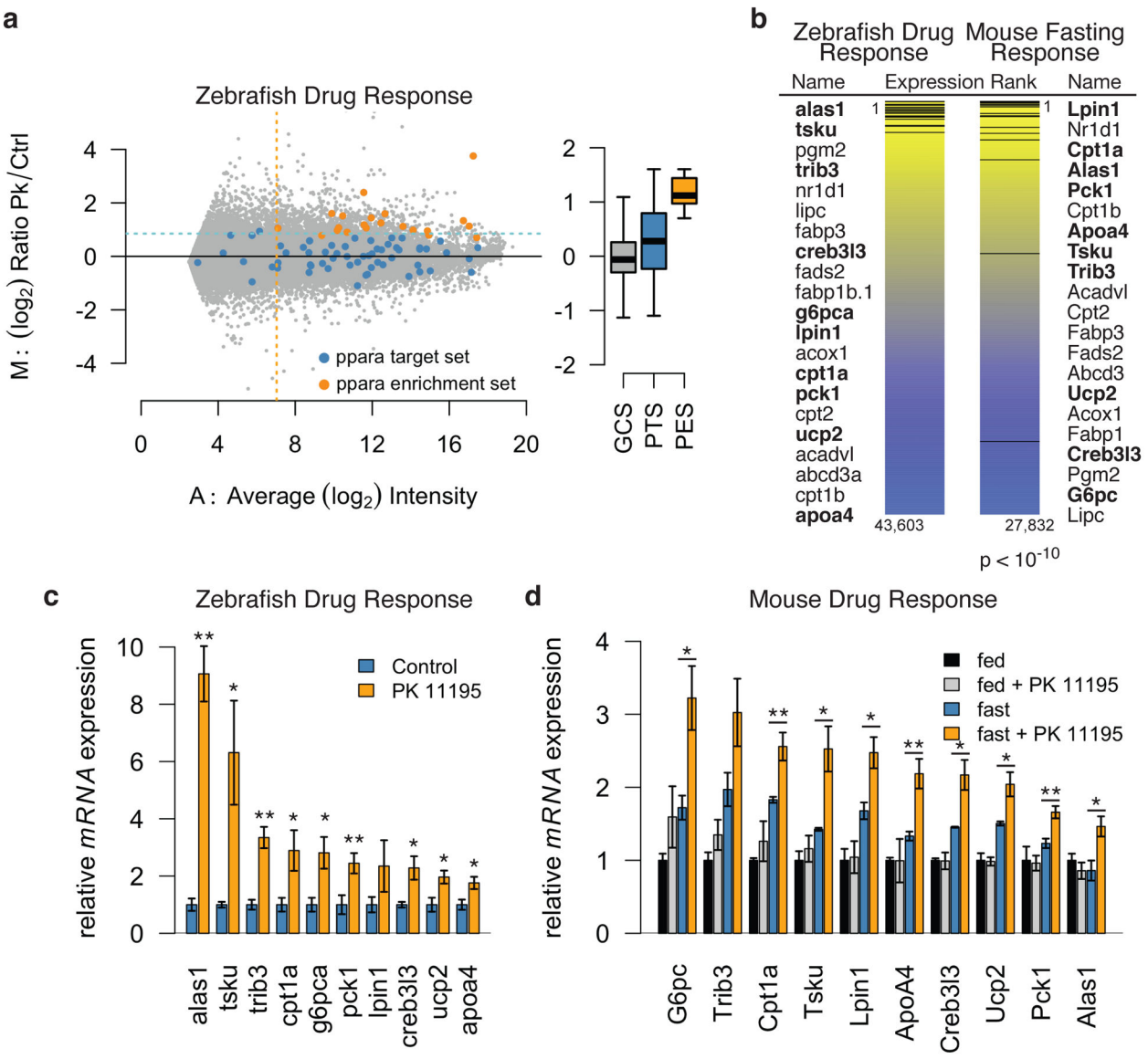

Figure 4. TSPO ligands induce a fasting-like energy state in the liver

(**a**) MA-scatterplot of a microarray comparison of liver tissue of PK 11195 and vehicle treated zebrafish. PK 11195 induces expression of a Ppar-α target gene set (PTS, blue). A subset of this gene cluster, the Ppar-α enrichment set (PES, orange), shows enriched expression in the top ranks of differentially regulated genes compared to all genes (Gene comparison set, GCS, grey) (control vs. 10μM PK 11195 from 4 to 6 dpf, n=2/condition of ~ 20 livers). Orange dashed line, median value of the average $\log_2$ signal intensity; blue dashed line, 90th percentile of all genes. (**b**) The 21 members of the PES gene set are also enriched at the top of the list of differentially regulated genes in mouse liver after a long physiological fast as shown by a Kolmogorov-Smirnov (K-S) statistic for cumulative distribution probability: Rank sorting of differentially regulated genes in fasted vs. fed mouse livers (C57BL/6, Standard Diet, n=3 microarray comparisons, 24h fast vs. fed) shows a significant enrichment of 19 out of the 21 PES orthologues [$p < 10^{-10}$ by K-S statistic for

all 21 genes]. Every horizontal black line marks one of the displayed genes rank sorted from top to bottom; yellow, up-regulated genes; blue, down-regulated genes. **(c)** qPCR analysis of PES genes in zebrafish livers (control vs. 10μM PK 11195, 6 dpf, n=5/condition) and **(d)** mouse livers (fed vs. fast; n = 3/condition, and fast + vehicle vs. fast + 2×5mg/kg bw PK 11195; 8h fast; n=6/condition; SD; 11–12 weeks male C57BL/6). *$p < 0.05$, **$p < 0.01$; two-tailed t-test. Data are represented as mean values ± s.e.m..

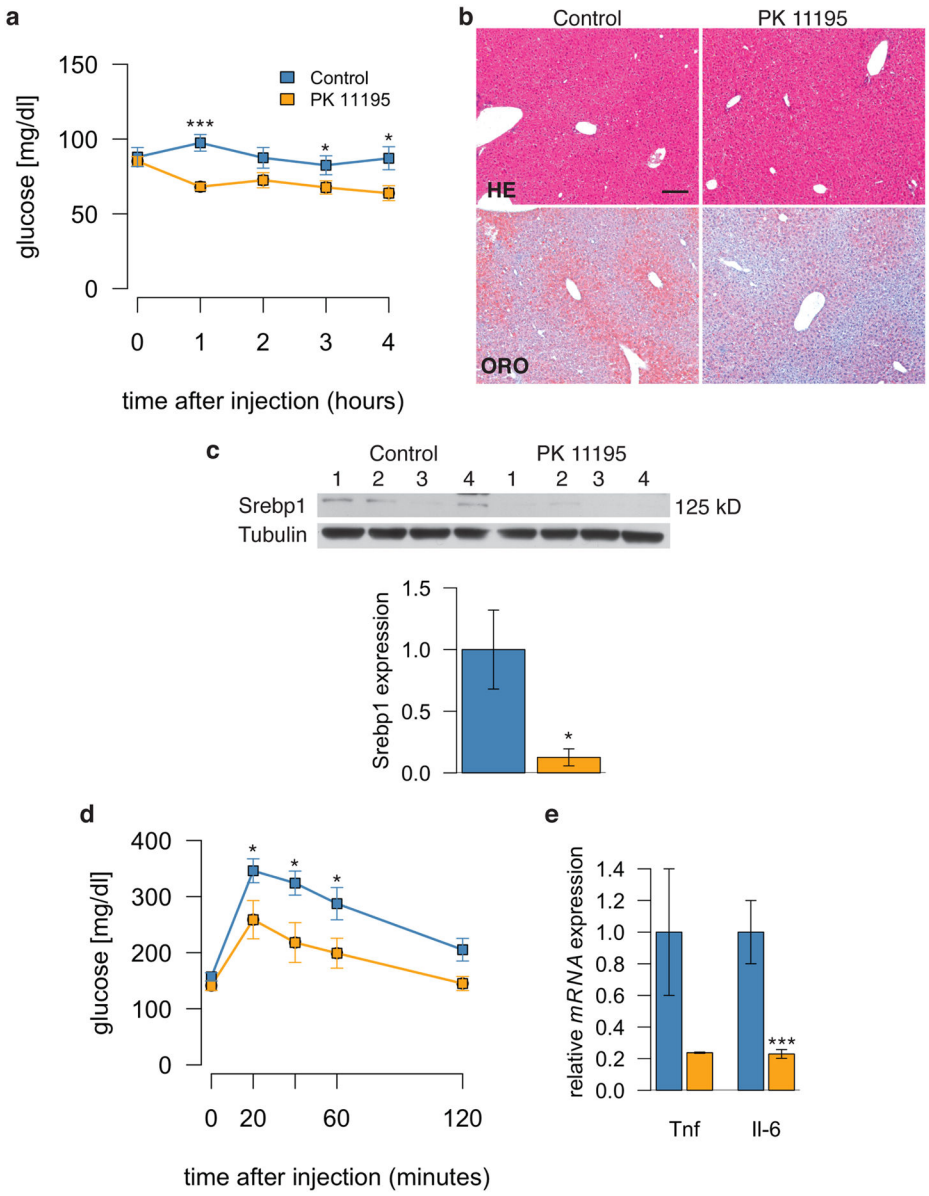

Figure 5. PK 11195 improves hepatosteatosis and glucose tolerance in diet-induced obese mice

(**a**) Hypoglycemic effects of PK 11195 treatment in fasted mice (1mg/kg bw PK 11195 in saline, standard diet, n=6/condition, 24h fast). (**b**) Representative images of Hematoxylin-Eosin (HE) and Oil-Red O (ORO) stained livers after 5 weeks of vehicle or PK 11195 treatment in diet-induced obese mice (1mg/kg bw PK 11195, s.c. injections for five days per week, n=5/condition, HFD from 10 to 19 weeks, start of intervention at 14 weeks). ORO staining shows reduced lipid accumulation in livers of the PK 11195 treatment group. Scale bar, 100μm (**c**) Srebp-1a protein levels are reduced in the liver in response to PK 11195 treatment (See Supplementary Figure 9 for uncut gels). (**d**) At four weeks of treatment, mice were subjected to an i.p. glucose tolerance test after a 6h fast. Two additional injections of PK 11195 (2mg/kg bw) were administrated at 8 am and 1h prior to the glucose challenge at 2 pm. PK 11195 treated animals show a significantly improved glucose tolerance (20min,

P=0.029; 40min, P=0.015; 60min, P=0.032; 120min, P=0.025). (**e**) mRNA transcript levels were quantified by qPCR for two pro-inflammatory markers, TNFα and Il-6, from livers of control and PK 11195 treated mice (from (**b**), n = 4/condition). *P < 0.05; **P < 0.01; ***P < 0.001; two-tailed t-test. All data are represented as mean values ± s.e.m..

Table 1

Drugs identified to modulate gluconeogenesis in zebrafish larvae

Name	Drug Class	Screening Phenotype	P-value (*pck1:*Luc2|glucose)	Experimental effects related to energy metabolism	Clinical effects related to energy metabolism
Isoprenaline	Beta-adrenergic agonist	*pck1* ++ Glucose +++	<0.0001|0.007	Sympathomimetic stimulation of energy metabolism[17,31]	Catecholamine-induced lipolysis, hyperglycemia, glycolysis and gluconeogenesis[32,33]
Formoterol			<0.0001|<0.0001		
Budenoside	Glucocorticoid	*pck1* + Glucose ++	<0.0001|0.005	Glucocorticoid-induced hepatosteatosis and insulin resistance in mice[34]	Iatrogenic diabetes, hepatic steatosis and increased cardiovascular risk[35].
Beclomethasone			0.0002|0.0005		
Dexamethasone			<0.0001|0.0002		
Clozapine	Atypical antipsychotic	*pck1* +++ Glucose +	0.0002|0.031	Diverse effects on glucose and energy metabolism in animal models[36,37]	Increased risk of diabetes and increased cardiovascular events[38]
Doxepine	Tricyclic antidepressant	*pck1* + Glucose +	0.003|0.005	Reduced insulin release from rat pancreata[39]. Acute hypo- and chronic hyperglycemia in rabbits[40].	Increased risk of diabetes and cardiovascular events[41]
Clomipramine			<0.0001|0.001		
Fluoxetine	SSRI	*pck1* ++ Glucose ±	0.001|0.035	Reduced lipid storage in *C. elegans*[42]	Acute weight loss[43]; Increased risk of diabetes[43,44]
PK 11195	TSPO Ligand	*pck1* ++ Glucose −	<0.0001|0.0097	Chemosensitizing effects to starvation-induced apoptosis in cancer cell lines[19]	N/A

Effect on *pck1:*Luc2 activity and glucose levels (*pck1*:Luc2 [$\log_2$-fold change]|glucose [pmol/larvae]):

− reduced (<−1|< 600; ± unchanged; + mild increase (> 1|> 900); ++ medium increase (> 1.5|> 1200); +++ strong increase (> 3|> 1500).